Balbekov (Tetra) Ring

Simulation Results in COSY

K. Makino
University of Illinois at Urbana-Champaign

Collaboration with:
M. Berz, C.O. Maidana (Michigan State University)

Supported by the Illinois Consortium for Accelerator Research,
the U.S. Department of Energy,
the NSF and the Alfred P. Sloan Foundation

See : ICAP 2002 Proceedings

Muon Beam Ring Cooler by V. Balbekov
(Pictures: Courtesy of Balbekov)

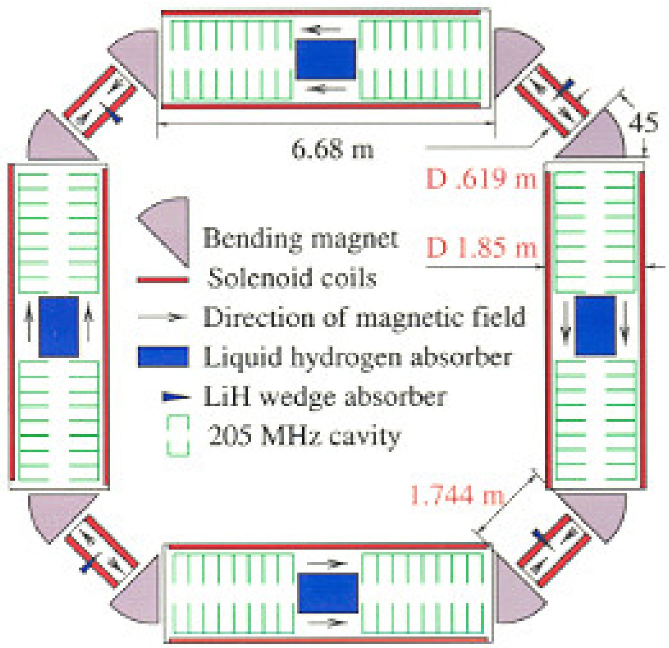

Circumference	36.963 m
Nominal energy at short SS and bends	250 MeV
Bending field	1.453 T
Norm. field gradient	0.5
Max. solenoid field	5.155 T
RF frequency	205.69 MHz
Accelerating gradient	15 MeV/m
LH_2 absorber length	128 cm
LiH wedge absorber	14 cm
Grad. of energy loss	0.75 MeV/cm

Figure 1: Layout and parameters of the solenoid based ring cooler.

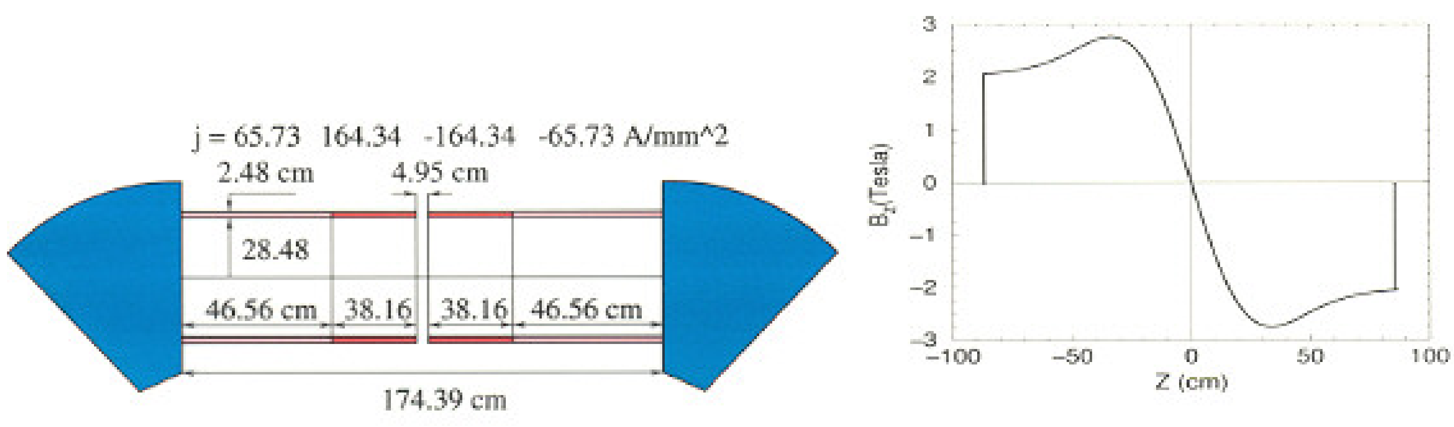

Map Method

- The transfer map is the flow of the system ODE.

$$\overrightarrow{z_f} = \mathcal{M}(\overrightarrow{z_i}, \vec{\delta})$$

- The Differential Algebraic (DA) method allows the computation and manipulation of maps efficiently and elegantly.
- For a repetitive system, only one cell has to be computed. Thus, much faster than tracking codes.
- The Normal Form method can be used for analysis of nonlinear behavior.

The Particle Optical Equations of Motion

$$
\begin{aligned}
x' &= a \cdot (1 + hx) \cdot \frac{p_0}{p_z} \\
y' &= b \cdot (1 + hx) \cdot \frac{p_0}{p_z} \\
l' &= (1 + \delta_m) \cdot (1 + hx) \cdot \frac{1 + \eta}{1 + \eta_0} \cdot \frac{p_0}{p_z} \\
a' &= \left((1 + \delta_m) \cdot \frac{1 + \eta}{1 + \eta_0} \cdot \frac{p_0}{p_z} \cdot \frac{E_x}{\chi_{E0}} - \frac{B_y}{\chi_{M0}} + b \cdot \frac{p_0}{p_z} \cdot \frac{B_z}{\chi_{M0}} \right) \\
&\quad \cdot (1 + hx) \cdot (1 + \delta_z) + h \cdot \frac{p_z}{p_0} \\
b' &= \left((1 + \delta_m) \cdot \frac{1 + \eta}{1 + \eta_0} \cdot \frac{p_0}{p_z} \cdot \frac{E_y}{\chi_{E0}} + \frac{B_x}{\chi_{M0}} - a \cdot \frac{p_0}{p_z} \cdot \frac{B_z}{\chi_{M0}} \right) \\
&\quad \cdot (1 + hx) \cdot (1 + \delta_z)
\end{aligned}
$$

$$
\begin{aligned}
\chi_{E0} &= \frac{p_0 \cdot v_0}{z_0 e}, \; \chi_{M0} = \frac{p_0}{z_0 e} \\
\eta &= \left(\frac{K_0 \cdot (1 + \delta_k) - z_0 \cdot e \cdot (1 + \delta_z) \cdot V(x, y, s)}{m_0 c^2 \cdot (1 + \delta_m)} \right) \\
\frac{p_z}{p_0} &= \sqrt{(1 + \delta_m)^2 \cdot \frac{\eta(2 + \eta)}{\eta_0(2 + \eta_0)} - a^2 - b^2}
\end{aligned}
$$

$$a = \frac{p_x}{p_0} \quad , \; b = \frac{p_y}{p_0}$$

DA Fixed Point Theorem

Differential Algebra ${}_nD_v$: in v variables up to order n.

Definition (Depth) To any element $[f] \in {}_nD_v$ we define the depth

$$\lambda([f]) = \begin{cases} \text{Order of first nonvanishing derivative of } f & \text{if } [f] \neq 0 \\ n+1 & \text{if } [f] = 0 \end{cases}.$$

Definition (DA Contracting Operator) Let $\mathcal{O}$ be an operator on the set $M \subset {}_nD_v^m$. $\mathcal{O}$ is contracting on M if for any $\vec{a}, \vec{b} \in M$ with $\vec{a} \neq \vec{b}$,

$$\lambda(\mathcal{O}(\vec{a}) - \mathcal{O}(\vec{b})) > \lambda(\vec{a} - \vec{b}).$$

Remark: Practically this means that after application of $\mathcal{O}$, the derivatives in $\vec{a}$ and $\vec{b}$ agree to a higher order than before application of $\mathcal{O}$.

Example: The antiderivation ∂_k^{-1}.

Theorem (DA Fixed Point Theorem) *Let $\mathcal{O}$ be a contracting operator on $M \subset {}_nD_v$ that maps M into M. Then $\mathcal{O}$ has a unique fixed point $a \in M$ that satisfies the fixed point problem*

$$a = \mathcal{O}(a).$$

Moreover, let a_0 be any element in M. Then the sequence

$$a_k = \mathcal{O}(a_{k-1}) \textit{ for } k = 1, 2, ...$$

converges in finitely many steps, at most $(n+1)$ steps, to the fixed point a.

DA Fixed Point PDE Solvers

The **DA fixed point theorem** allows to **solve PDEs iteratively** in **finitely many steps** by rephrasing them in terms of a fixed point problem.

Consider the rather general PDE

$$a_1 \frac{\partial}{\partial x}\left(a_2 \frac{\partial}{\partial x} V\right) + b_1 \frac{\partial}{\partial y}\left(b_2 \frac{\partial}{\partial y} V\right) + c_1 \frac{\partial}{\partial z}\left(c_2 \frac{\partial}{\partial z} V\right) = 0,$$

where a_i, b_i, c_i are functions of x, y, z.

The PDE is re-written as

$$\begin{aligned} V &= V\big|_{y=0} + \int_0^y \frac{1}{b_2}\left(b_2 \frac{\partial V}{\partial y}\right)\bigg|_{y=0} \\ &\quad - \int_0^y \frac{1}{b_2} \int_0^y \left(\frac{a_1}{b_1}\frac{\partial}{\partial x}\left(a_2 \frac{\partial V}{\partial x}\right) + \frac{c_1}{b_1}\frac{\partial}{\partial z}\left(c_2 \frac{\partial V}{\partial z}\right)\right) dy dy, \end{aligned}$$

in **fixed point form**.

Assume the derivatives of V and $\partial V/\partial y$ with respect to x and z are **known in the plane** $y = 0$. Then the right hand side is **contracting** with respect to y, and the various orders in y can be **iteratively** calculated by mere iteration.

Analytical Field on Axis for a thick Solenoid

$$B_S(s)=\frac{\mu_0 In}{2(R_2-R_1)}\left\{s\log\left(\frac{R_2+\sqrt{R_2^2+s^2}}{R_1+\sqrt{R_1^2+s^2}}\right)-(s-l)\log\left(\frac{R_2+\sqrt{R_2^2+(s-l)^2}}{R_1+\sqrt{R_1^2+(s-l)^2}}\right)\right\}$$

$$V(s)=\frac{\mu_0 In}{4(R_2-R_1)}\left\{s^2\log\left(\frac{R_2+\sqrt{R_2^2+s^2}}{R_1+\sqrt{R_1^2+s^2}}\right)-(s-l)^2\log\left(\frac{R_2+\sqrt{R_2^2+(s-l)^2}}{R_1+\sqrt{R_1^2+(s-l)^2}}\right)\right.$$

$$\left.+R_2\sqrt{R_2^2+s^2}-R_1\sqrt{R_1^2+s^2}-R_2\sqrt{R_2^2+(s-l)^2}+R_1\sqrt{R_1^2+(s-l)^2}\right\}$$

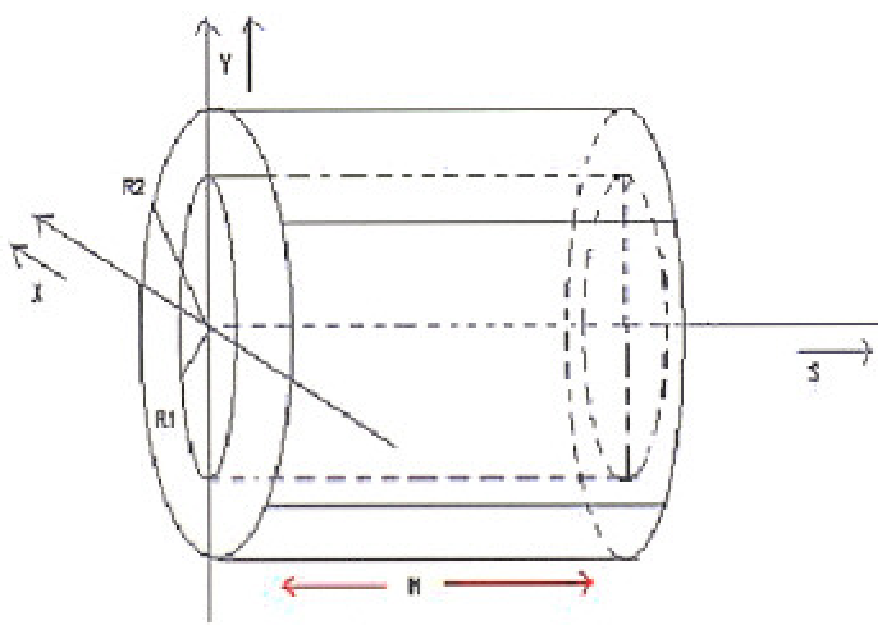

Balbekov Ring: Short Section

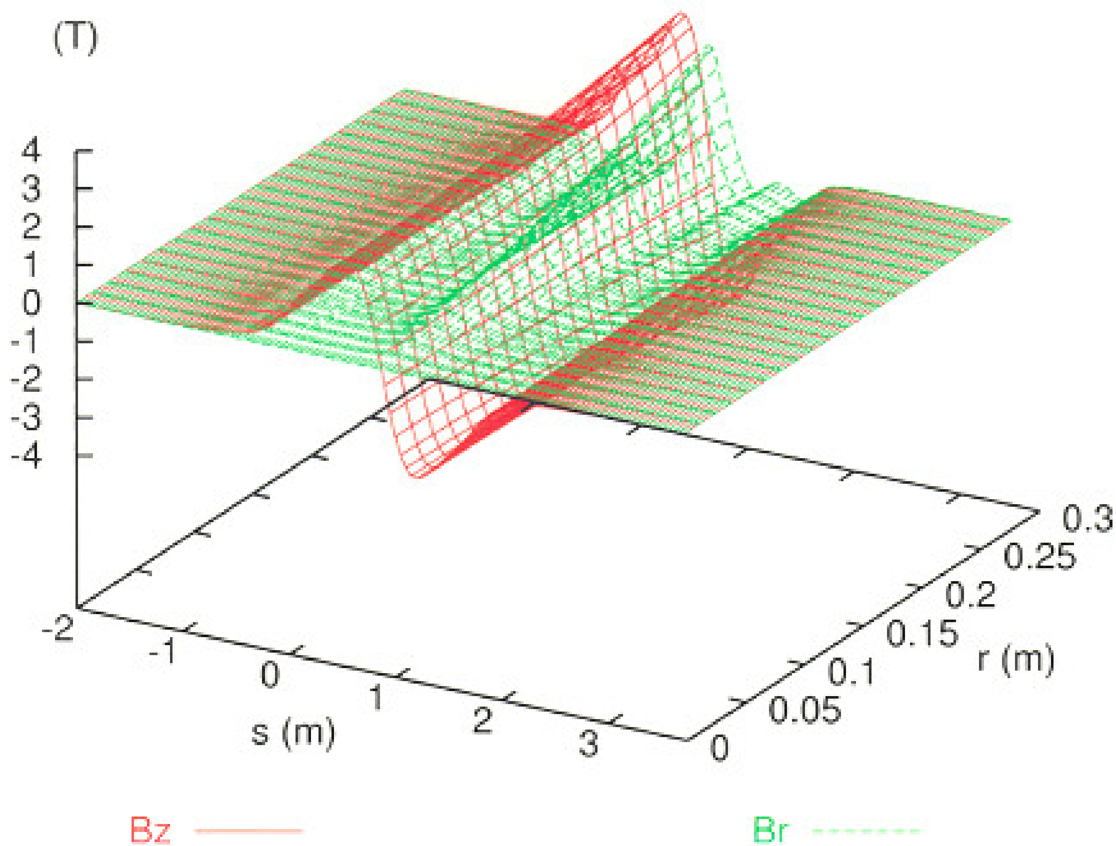

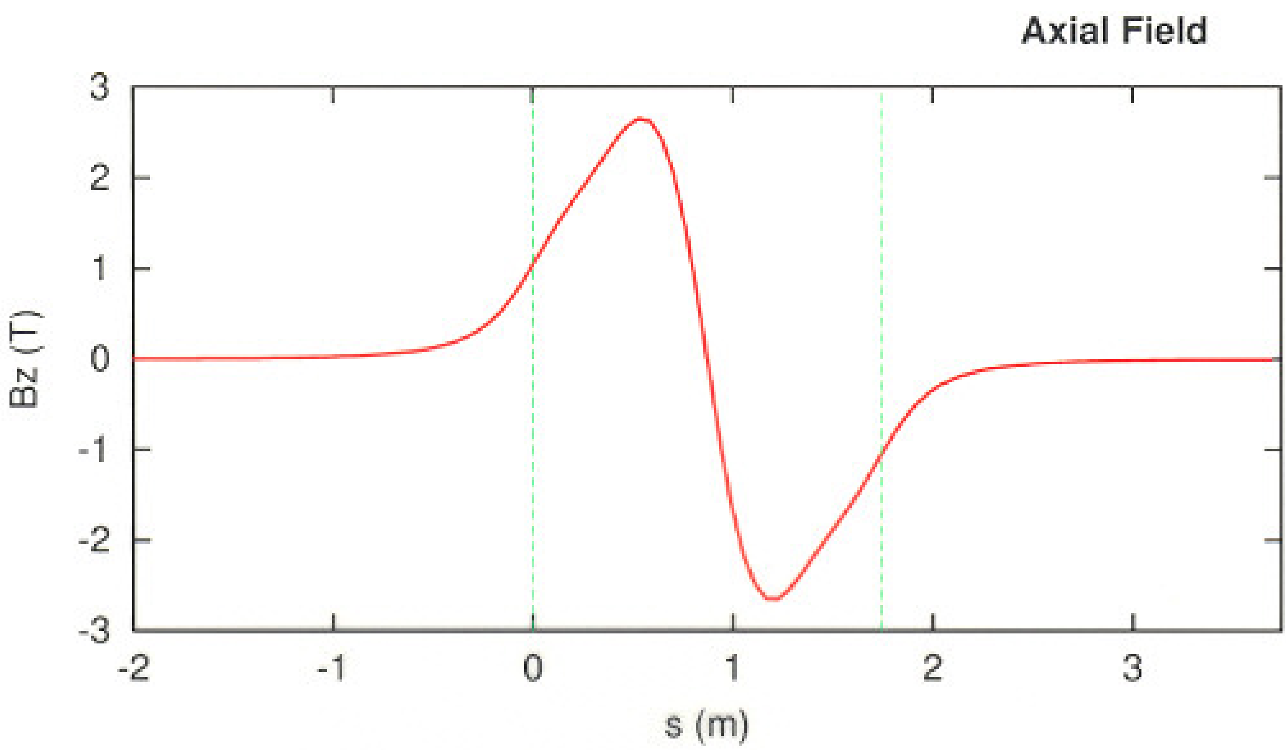

Kick Approximation V.S. COSY Computation

Short Section Kinetic Energy 250 MeV.

1) Transfer Map with **Kick** Approximation in the **Asymptotic** Fields

-0.1467136	-0.9637261	-0.2022731E-03	0.5845774E-04	1000
1.015304	-0.1467136	0.3060451E-11	-0.2022730E-03	0100
0.2022731E-03	-0.5845774E-04	-0.1467136	-0.9637261	0010
-0.3060451E-11	0.2022730E-03	1.015304	-0.1467136	0001
	... Omitted ...			
-2.968705	1.388108	1.284507	1.099203	5000
-12.74829	-1.191336	1.970436	4.189763	4100
-22.23560	-5.817135	-0.2996768	5.761626	3200

* The consistency was checked with linear matrices supplied by Balbekov.

2) Transfer Map with **Kick** Approximation in the **Realistic** Fields

0.3762572E-01	-0.9144481	0.1324007E-03	0.9123892E-05	1000
1.092008	0.3762572E-01	0.1216993E-10	0.1324008E-03	0100
-0.1324007E-03	-0.9123892E-05	0.3762572E-01	-0.9144481	0010
-0.1216993E-10	-0.1324008E-03	1.092008	0.3762572E-01	0001
	... Omitted ...			
-4.559878	2.194351	1.925709	2.734348	5000
-14.03917	1.790312	1.247951	8.100432	4100
-26.15120	-0.5027561	-4.741542	9.421870	3200

3) Transfer Map Computed with **Fringe** Fields by **COSY**

0.9113584E-02	-0.9101484	0.2707143E-04	-0.8741688E-06	1000
1.098631	0.9113584E-02	-0.1597370E-05	0.2707097E-04	0100
-0.2707143E-04	0.8741688E-06	0.9113584E-02	-0.9101484	0010
0.1597370E-05	-0.2707097E-04	1.098631	0.9113584E-02	0001
	... Omitted ...			
-4.919054	1.095873	0.6296333	1.603693	5000
-14.58589	0.6387705	-0.2037065	4.302134	4100
-24.12332	-1.227331	-3.197581	3.442199	3200

Muon Beam Ring Cooler by V. Balbekov
(Pictures: Courtesy of Balbekov)

Long Section

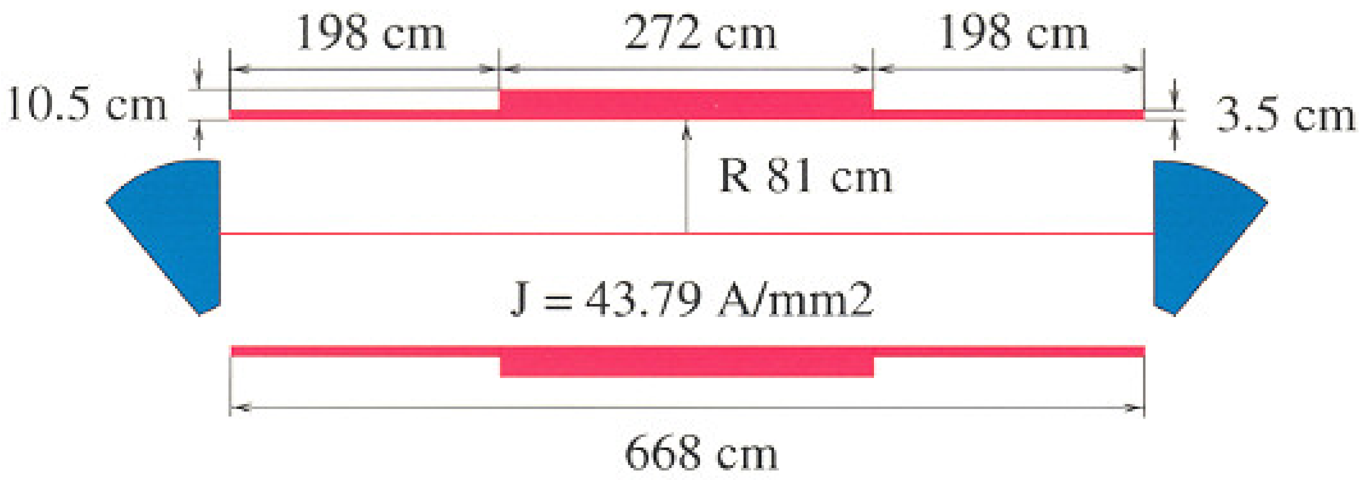

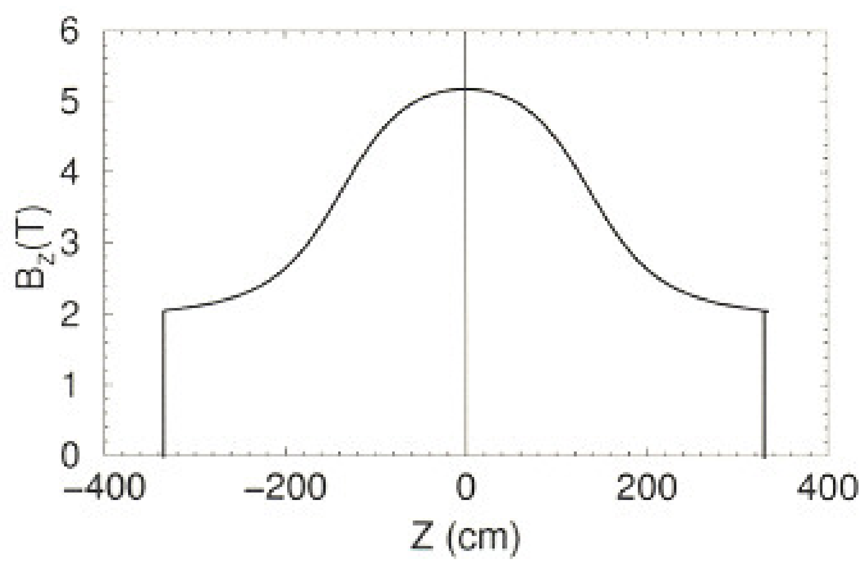

Axial Field with Infinitely Extended End Coils

Balbekov Ring: Long Section

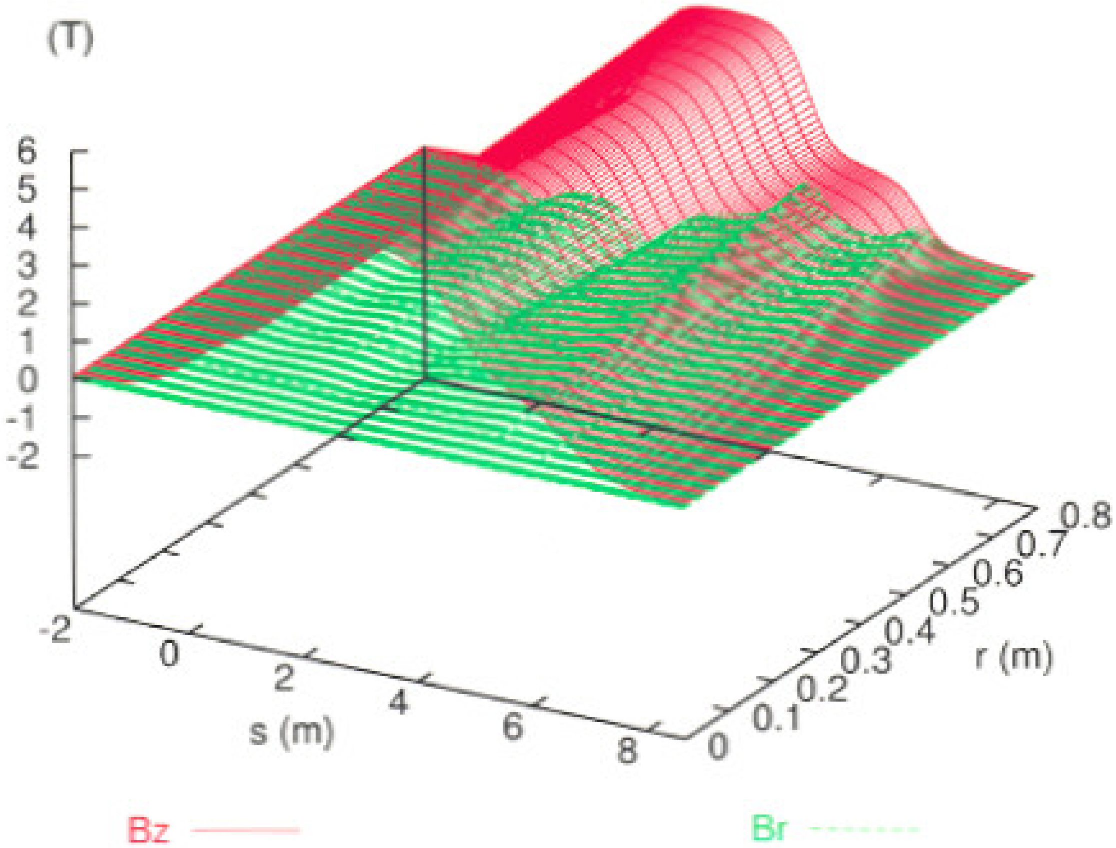

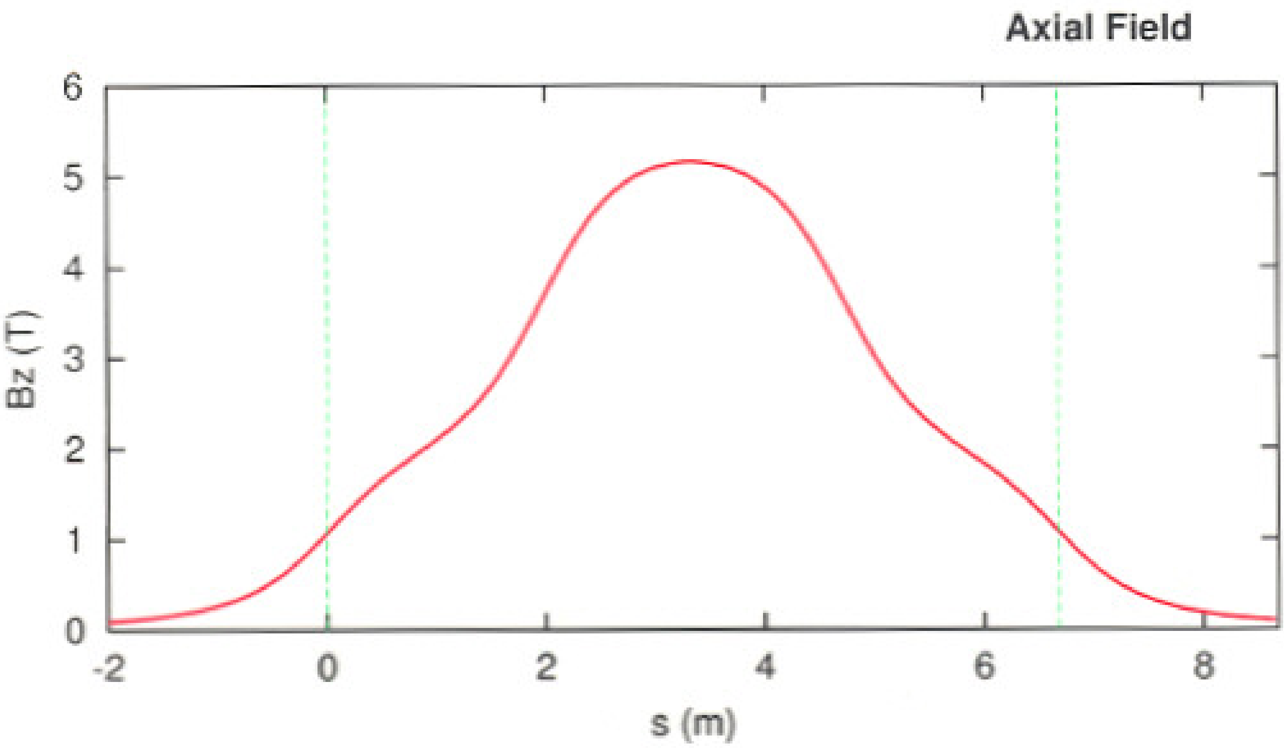

Balbekov's Kick Approximation V.S. COSY Computation

Long Section (Length 6.68m, Inner radius 81cm, Coil thickness 3.5cm to 10.5cm)

Linear Transfer Map with Balbekov's Kick Approximation (Full Aperture)

-0.1563521E-02	0.4816040E-01	-0.3071766E-01	0.9461698	1000
-0.5360646E-01	-0.1563561E-02	-1.053164	-0.3071766E-01	0100
0.3071766E-01	-0.9461698	-0.1563521E-02	0.4816040E-01	0010
1.053164	0.3071766E-01	-0.5360646E-01	-0.1563561E-02	0001

Linear Transfer Map Computed with Fringe Fields by COSY (Full Aperture)

0.2349601	0.7548866	0.8860107E-01	0.2030465	1000
-1.157433	0.2477034	-0.3113219	0.4122390E-01	0100
-0.8860107E-01	-0.2030465	0.2349601	0.7548866	0010
0.3113219	-0.4122390E-01	-1.157433	0.2477034	0001

Difference between the Kick Approximation and COSY with Smaller Aperture

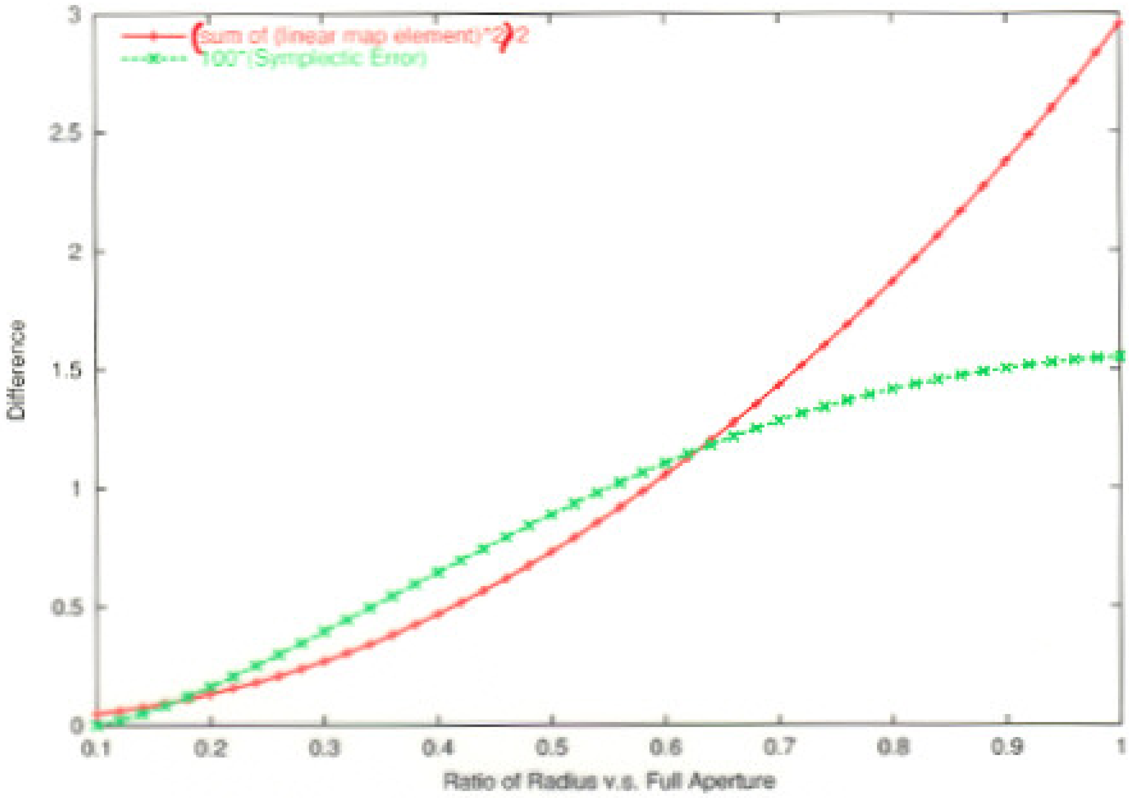

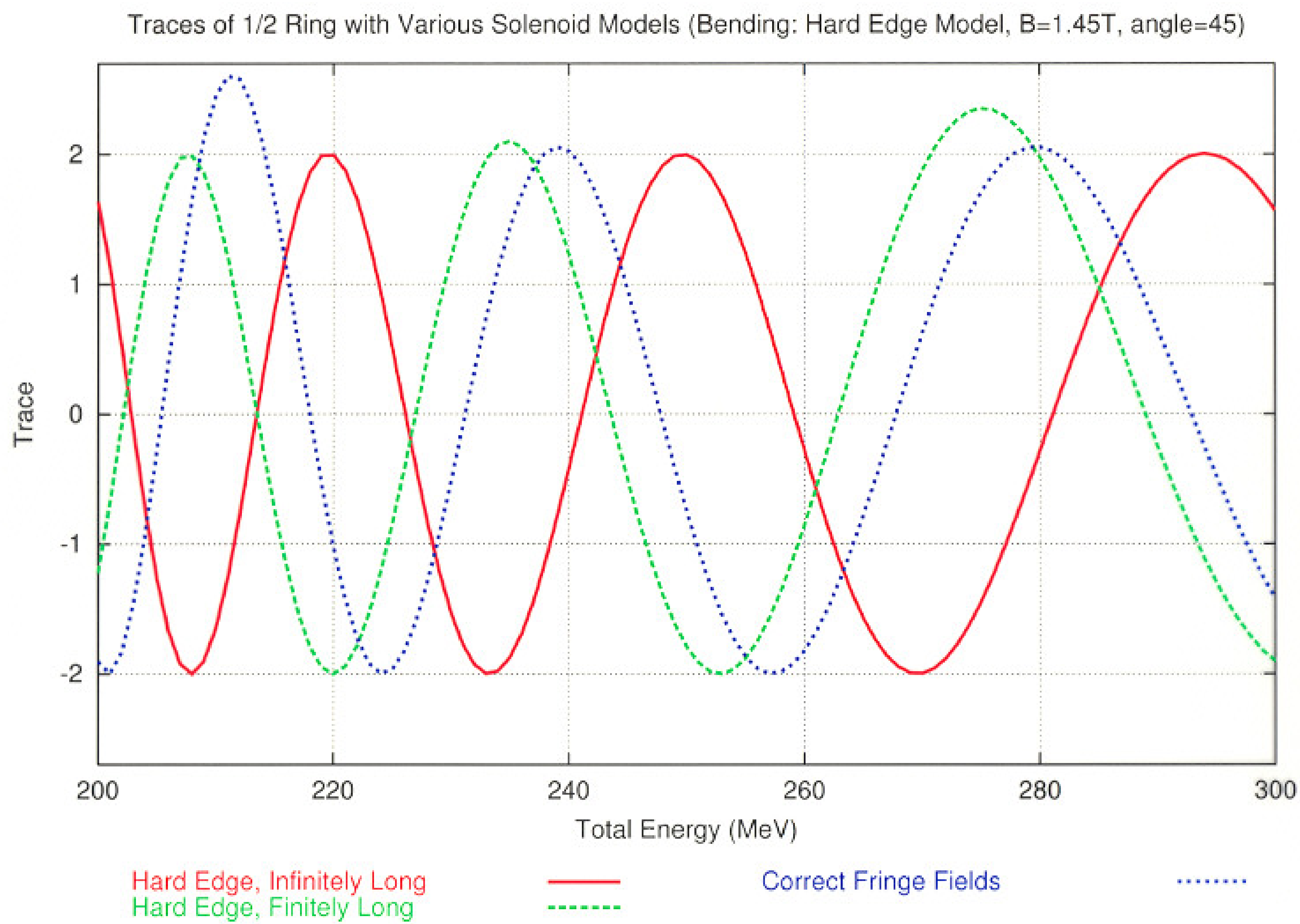
Traces of 1/2 Ring with Various Solenoid Models (Bending: Hard Edge Model, B=1.45T, angle=45)
Trace
2
1
0
-1
-2
200
220
240
260
280
300
Total Energy (MeV)
Hard Edge, Infinitely Long
Hard Edge, Finitely Long
Correct Fringe Fields

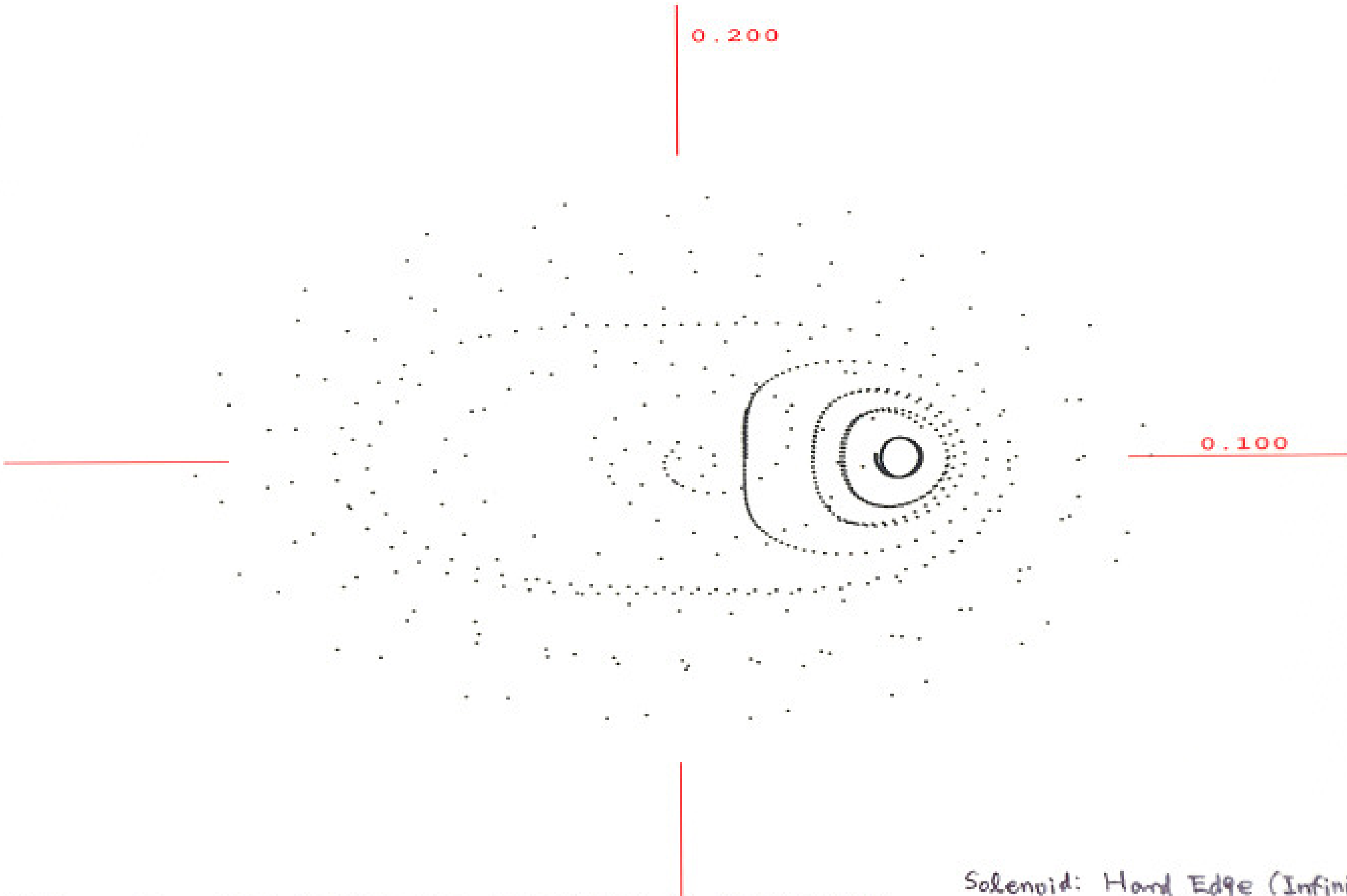

7-th order, 100 1/2 turns, Etot=250 1k FR 0 EXPO

Solenoid: Hard Edge (Infinitely Long)
Bending: Hard Edge

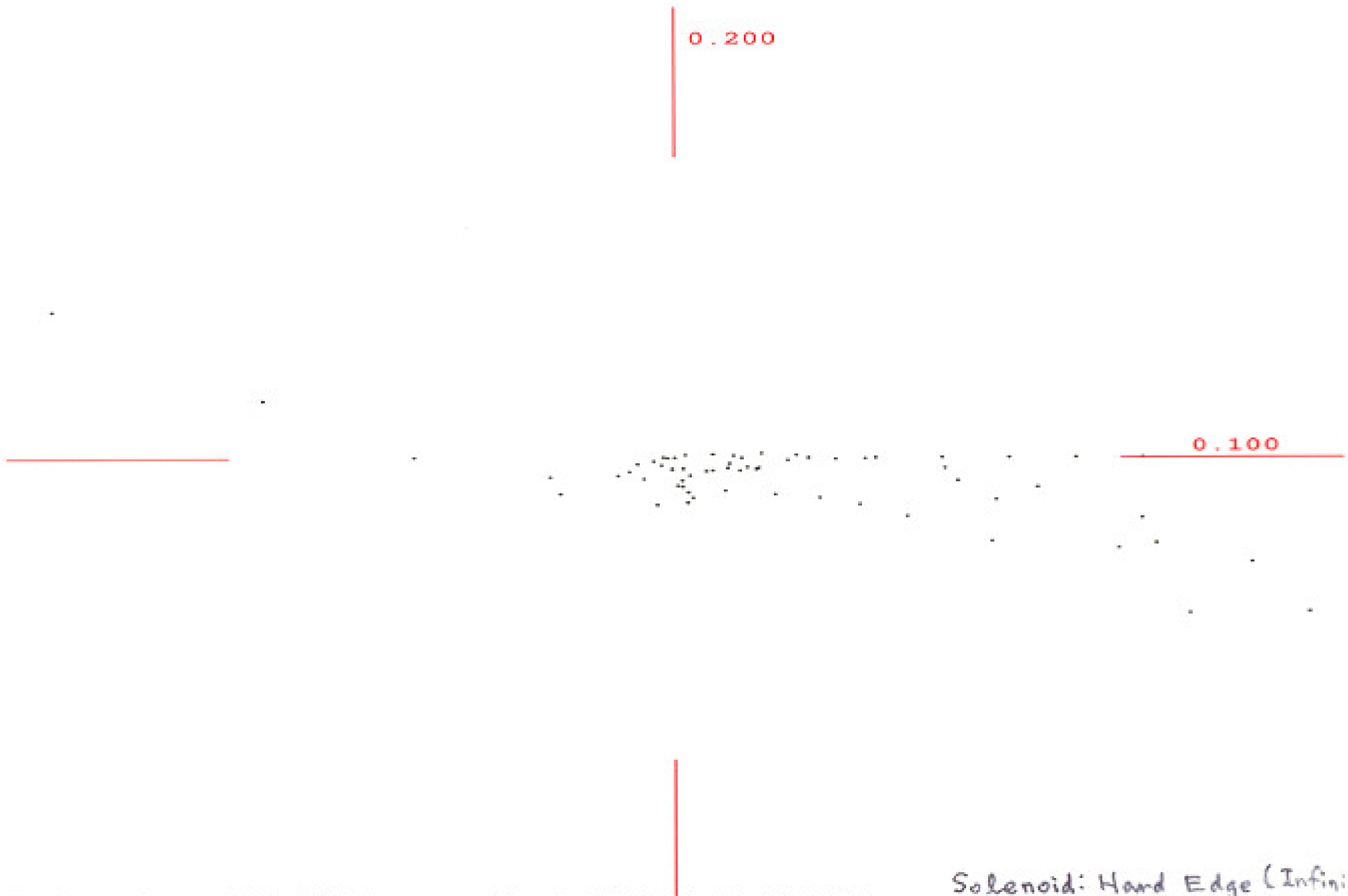

7-th order, 100 1/2 turns, Etot=250 1k FR 2 EXPO

Solenoid: Hard Edge (Infinitely Long)

Bending: with Fringe Fields

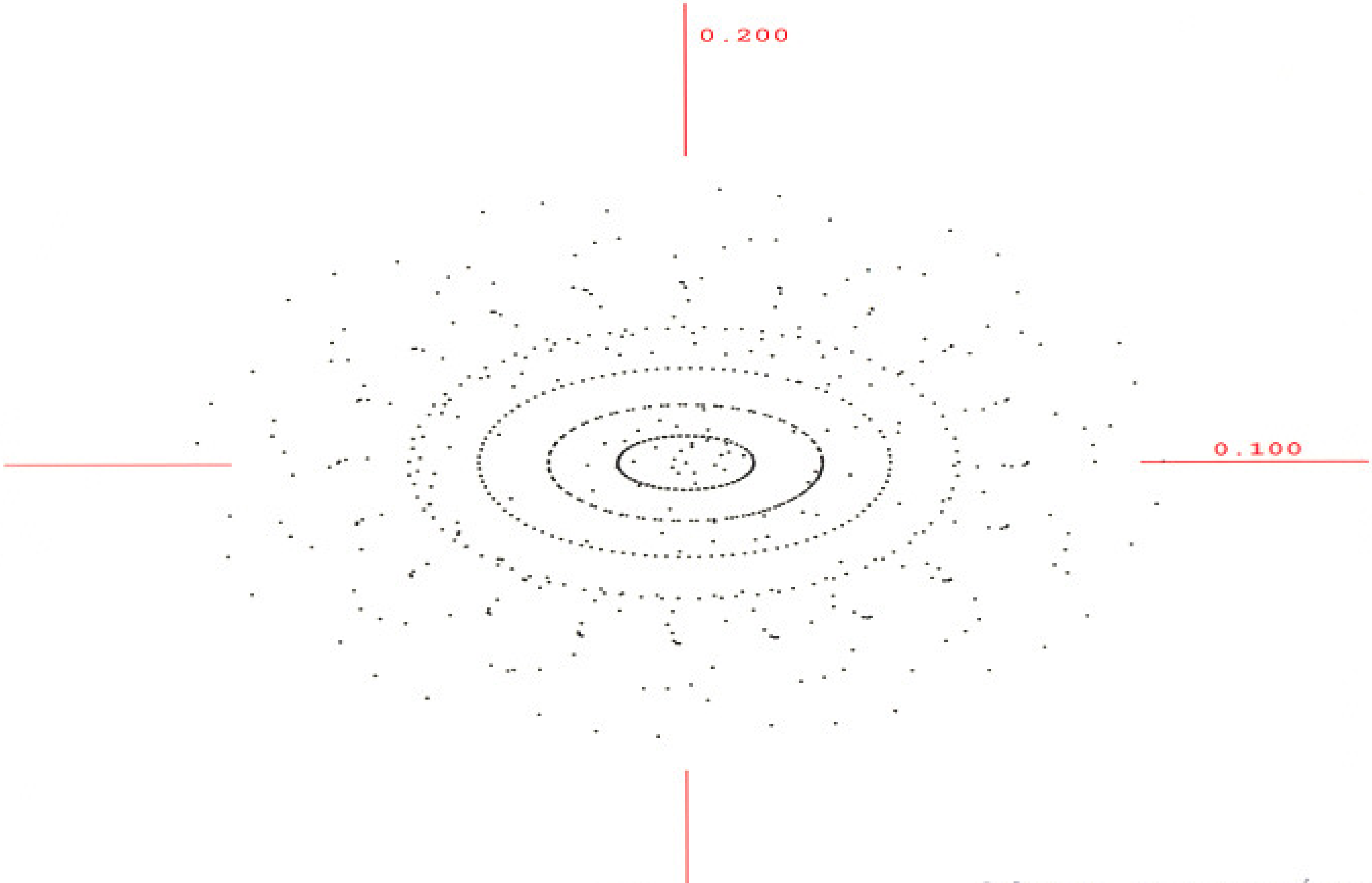

7-th order, 100 1/2 turns, Etot=249 1k FR 0 EXPO

Solenoid: Hard Edge (Infinitely Long)
Bending: Hard Edge

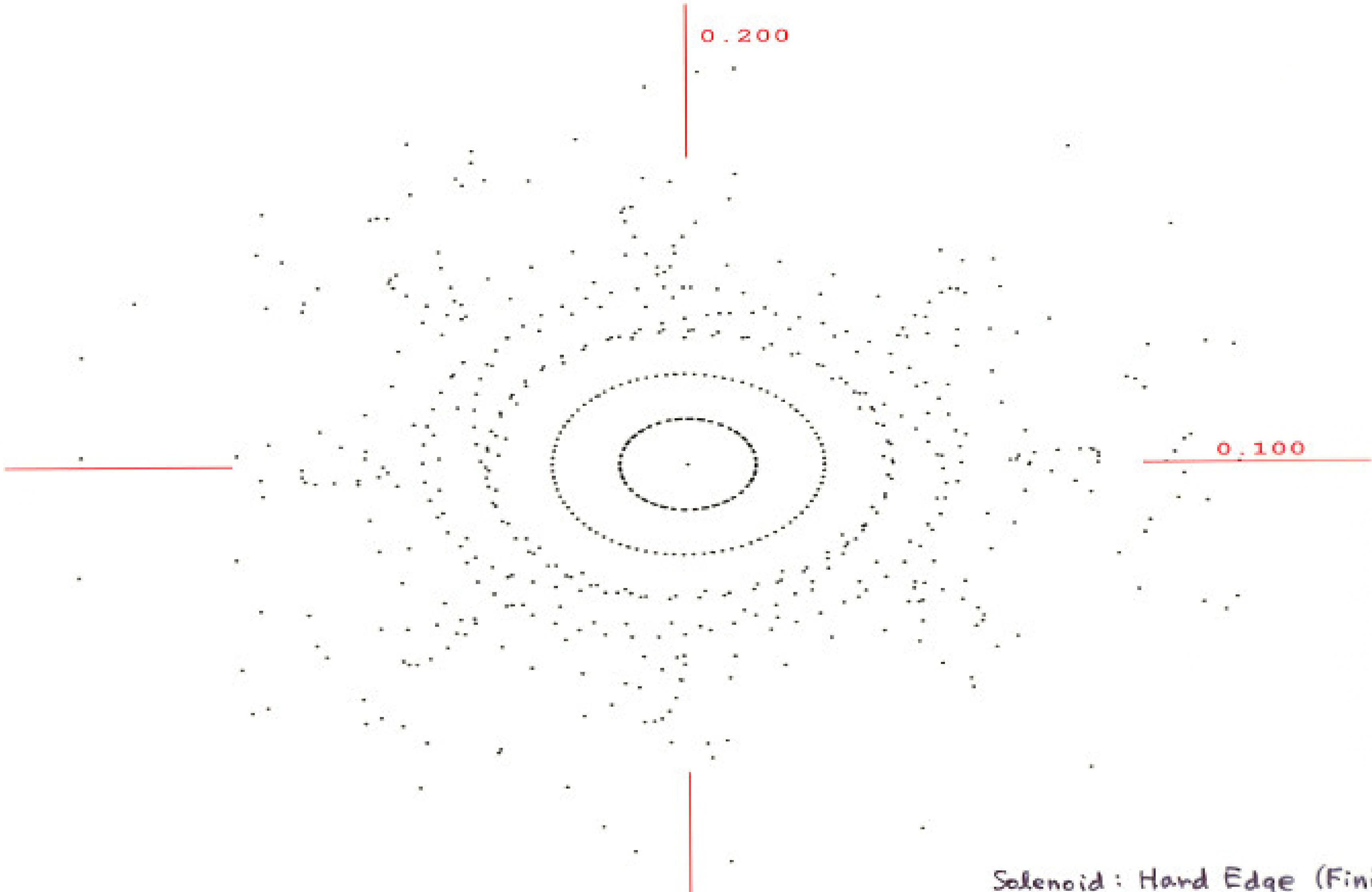

9-th order, 100 1/2 turns, Etot=250 2k FR 0

Solenoid : Hard Edge (Finitely Long)
Bending: Hard Edge

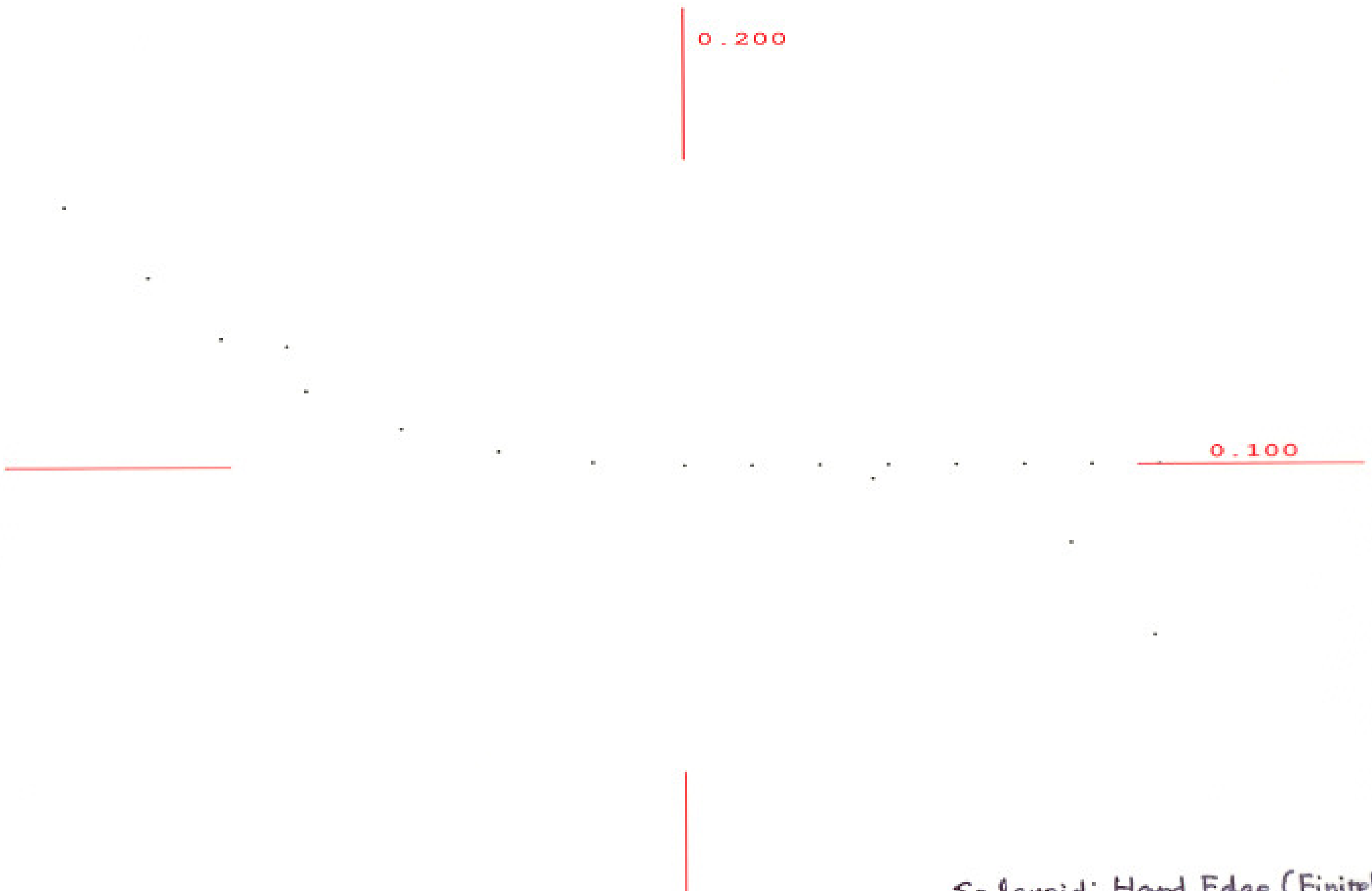

9-th order, 100 1/2 turns, Etot=250 2k FR 2

Solenoid: Hard Edge (Finitely Long)
Bending: with Fringe Fields

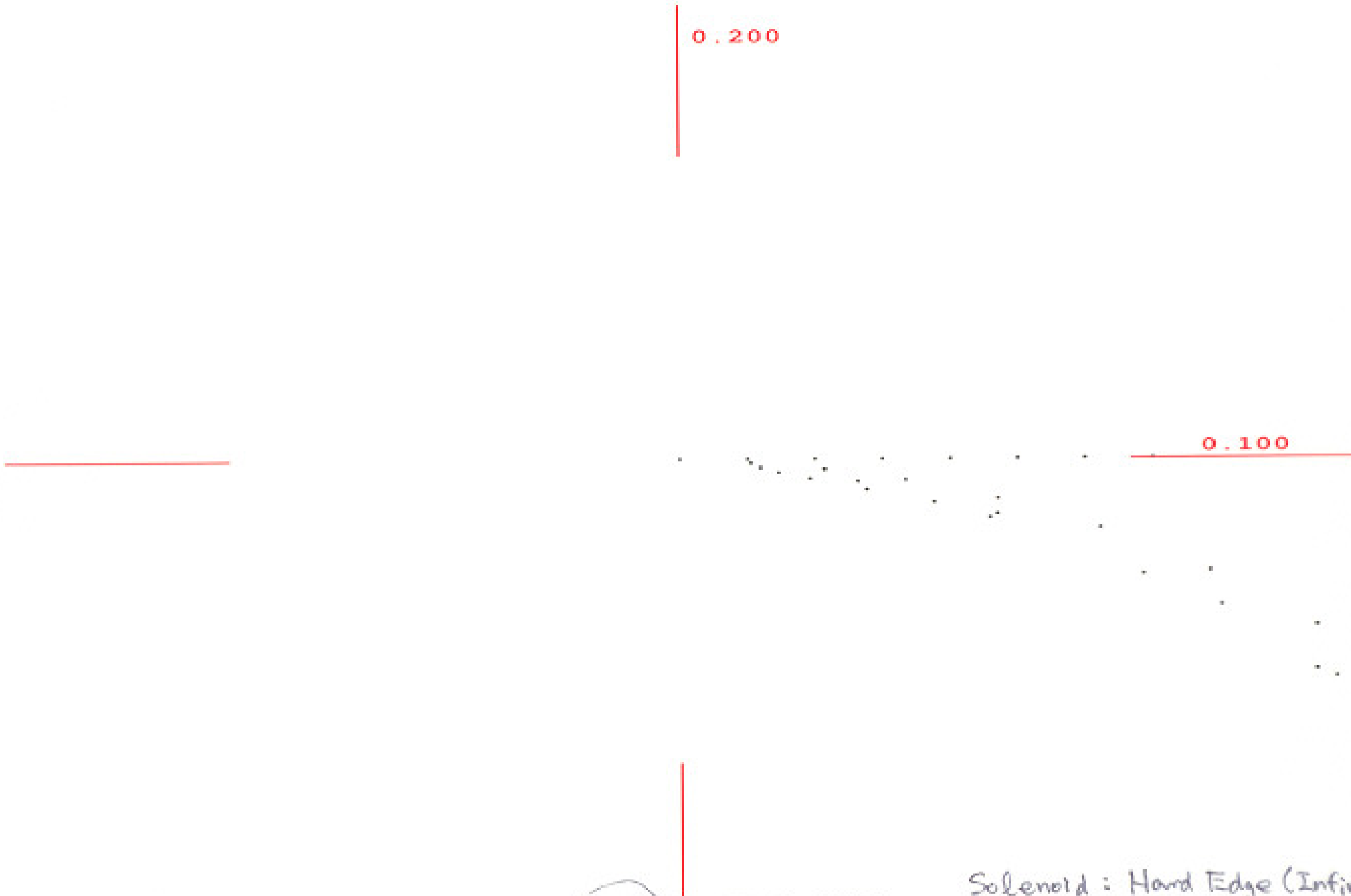

7-th order, 100 1/2 turns, Etot=249 1k FR 2 EXPO

Solenoid : Hard Edge (Infinitely Long)
Bending : with Fringe Fields

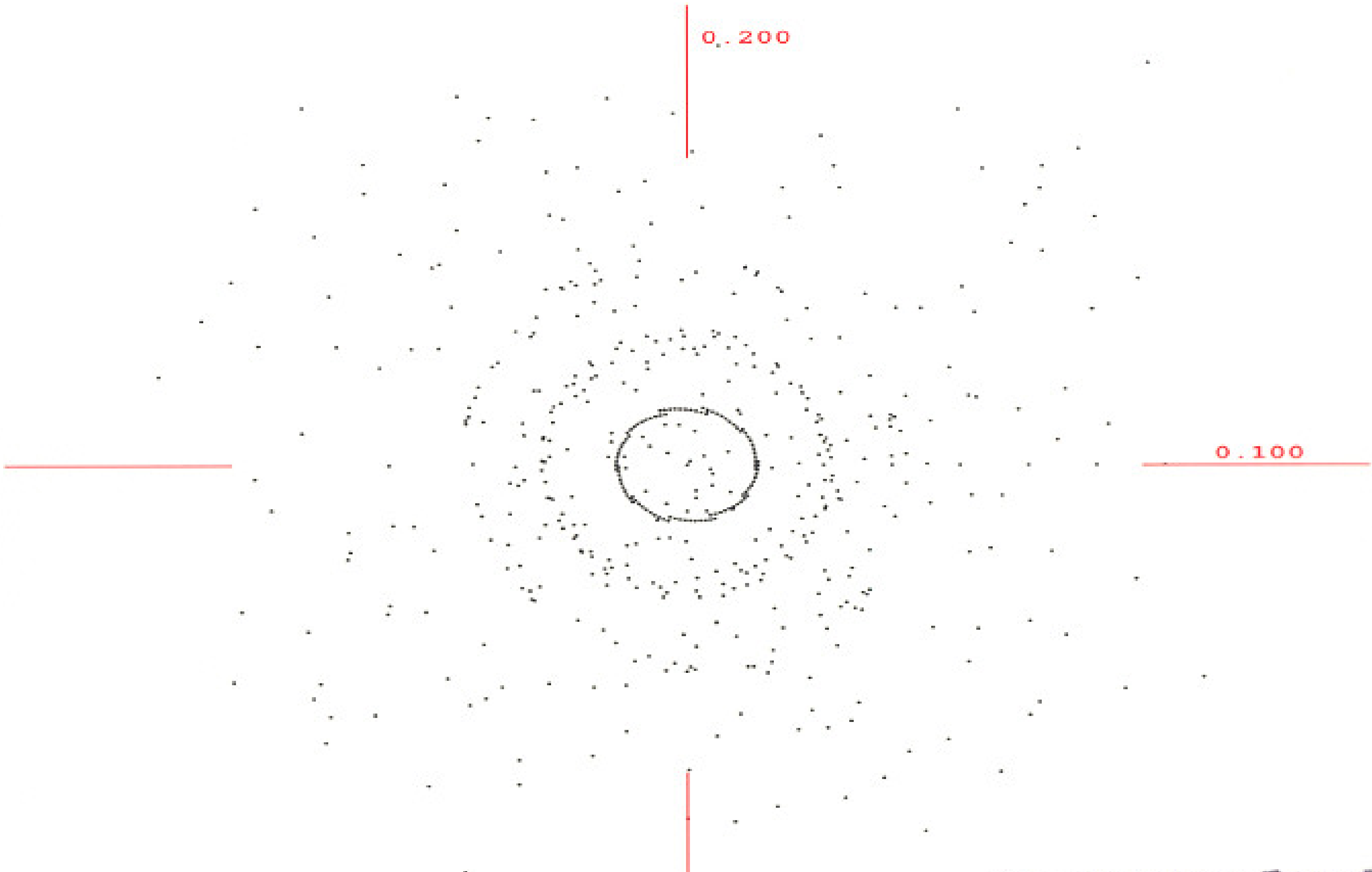

7-th order, 100 1/2 turns, Etot=250 3s FR 0 EXPO

Solenoid: Correct Fringe Fields
Bending: Hard Edge

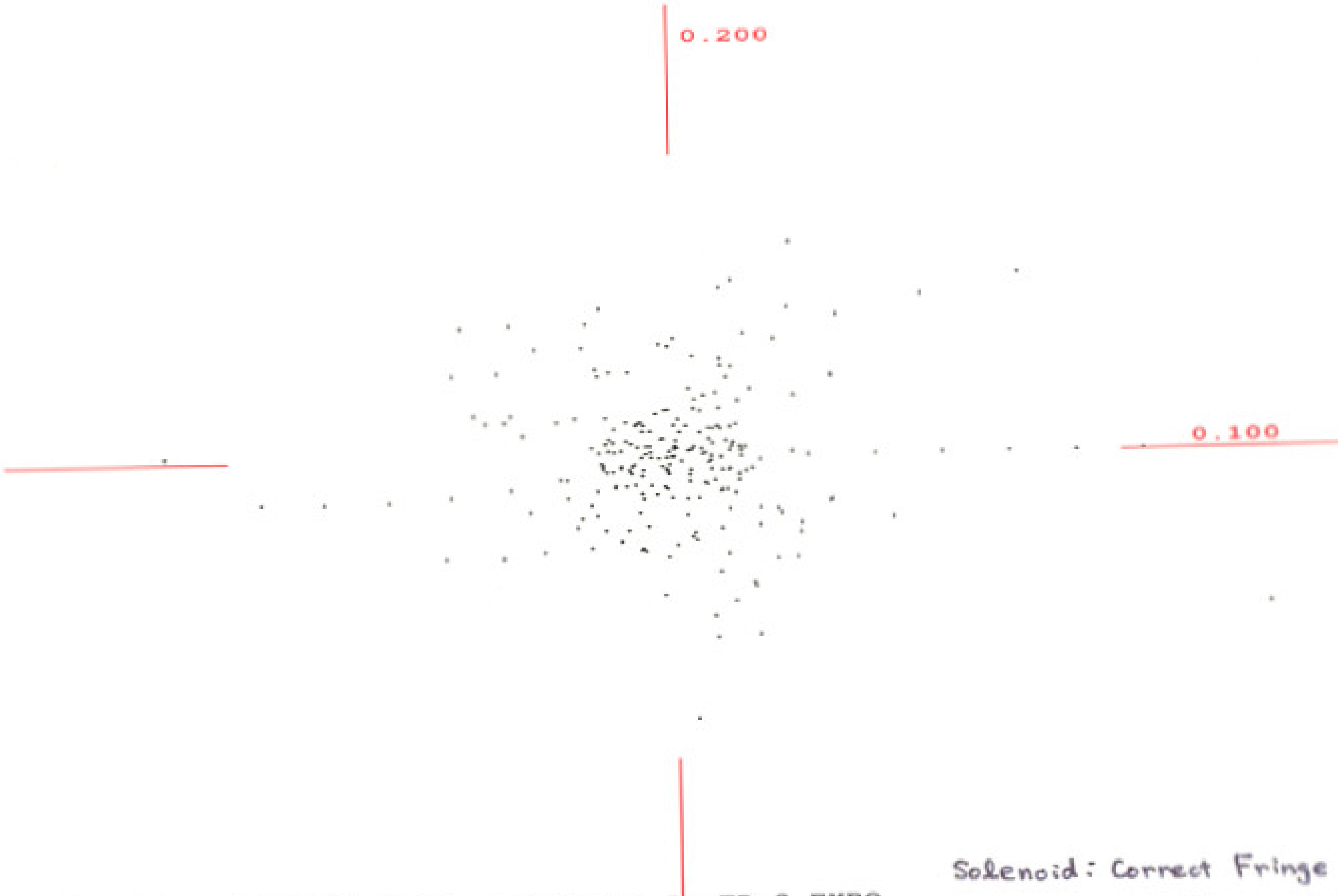

7-th order, 100 1/2 turns, Etot=250 3s FR 2 EXPO

Solenoid: Correct Fringe Fields
Bending: with Fringe Fields

Conclusion and Outlook

- There are strong resonance structures with /without FF.
- The FF effects have a dramatic impact on performance.

Next studies ....

- What is the impact of damping on the performance.